Observation of subcritical geodesic acoustic mode excitation in the Large Helical Device

T. Ido[1], K. Itoh[1,2], M. Lesur[3], M. Osakabe[1,4], A. Shimizu[1], K. Ogawa[1,4], M. Nishiura[5], I. Yamada[1], R. Yasuhara[1], Y. Kosuga[2], M. Sasaki[2], K. Ida[1,2], S. Inagaki[2], S. –I. Itoh[2], and the LHD Experiment Group[1]

[1]National Institute for Fusion Science, National Institutes of Natural Sciences, 322-6 Oroshi, Toki, Gifu 509-5292, Japan

[2]Research Institute for Applied Mechanics, Kyushu Univ., 6-1 Kasuga-koen, Kasuga, Fukuoka, 816-8580, Japan

[3]Institut Jean Lamour, UMR 7198 CNRS - Université de Lorraine, Campus Sciences, Bd des Aiguillettes, BP 70239, 54 506 VANDOEUVRE-LES-NANCY Cedex, France

[4]SOKENDAI(Grad. Univ. for Advanced Study), 322-6 Oroshi, Toki, Gifu 509-5292, Japan

[5]Graduate School of Frontier Sciences, Univ. of Tokyo, 5-1-5 Kashiwanohara, Kashiwa, Chiba, 277-8561, Japan

Abstract

Abrupt and strong excitation of a geodesic acoustic mode(GAM) has been found in the Large Helical Device (LHD), when the frequency of a chirping energetic particle-driven GAM (EGAM) approaches twice the GAM frequency. The temporal evolution of the phase relation between the abrupt GAM and the chirping EGAM is common in all events. The result indicates a coupling between the GAM and the EGAM. In addition, the nonlinear evolution of the growth rate of the GAM is observed, and there is a threshold in the amplitude of the GAM for the appearance of the nonlinear behavior. A threshold in the amplitude of the EGAM for the abrupt excitation of the GAM is also observed. According to a theory [M. Lesur, et al., Phys. Rev. Lett. **116**, 015003 (2016), K. Itoh, et al., Plasma Phys. Reports **42** 428 (2016)], the observed abrupt phenomenon can be

interpreted as the excitation of a subcritical instability of the GAM. The excitation of a subcritical instability requires a trigger and a seed with sufficient amplitude. The observed threshold in the amplitude of the GAM seems to correspond to the threshold in the seed, and the threshold in the amplitude of the EGAM seems to correspond to the threshold in the magnitude of the trigger. Thus, the observed threshold support the interpretation that the abrupt phenomenon is the excitation of a subcritical instability of the GAM.

1. Introduction

Understanding of particle and heat transport in magnetized plasmas is an important issue for designing nuclear fusion reactors with sufficient predictability. Since the transport is caused dominantly by fluctuations, understanding the properties of the fluctuations, especially the excitation conditions and the saturation level, is essential to assess the performance of plasmas.

Linear analysis of the excitation condition of instabilities provides a guide for the production of laboratory plasmas. However, the prediction of the onset of the instabilities is an open question, as reviewed in Ref.[1]. Especially, there is room to improve the understanding of sudden increase in the growth rate of instabilities, which is featured in phenomena such as sawtooth oscillation, or disruption in current-carrying toroidal plasmas and solar flares. In particular, the rate of change of the linear growth rate is limited by the rate of change of global equilibrium parameters, which is too

slow to explain the abrupt onset. This difficulty is known as the trigger problem and has been a challenge in laboratory plasmas and astro-plasmas for more than a couple of decades[1, 2]. One of the working hypotheses to understand the trigger problem is that of subcritical instability, which is driven nonlinearly in the linearly stable parameter region if the initial seed is sufficiently large. In magnetically confined plasmas, theoretical works have predicted several subcritical instabilities: current-diffusive interchange turbulence[3], magnetic island formation due to neoclassical tearing mode[4], and instabilities caused by kinetic nonlinearity including fast ion-driven instabilities[5, 6, 7, 8, 9, 10, 11, 12]. So far, however, there is no clear experimental result demonstrating the subcritical instabilities in plasmas.

Recently, the abrupt excitation of an geodesic acoustic mode(GAM) [13] has been found in magnetically confined toroidal plasmas in the Large Helical Device (LHD)[14]. This occurs in the presence of an energetic particle-driven GAM (EGAM)[15] with nonlinear temporal evolution of the frequency. The EGAMs have been widely observed in toroidal plasmas such as JET[16, 17], DIII-D[18], LHD[19, 20], JT-60U[21], ASDEX-Upgrade[22], and HL-2A[23]. The frequency of the EGAM often chirps up quickly, and the time scale (~ several ms) is much faster than the time scale of change in global equilibrium parameters. The evolution corresponds to the evolution of structures in the velocity space of the energetic particle described by Berk-Briezman's model[24]. However, the time scale of the abrupt phenomenon observed in this study is much faster than that of the

EGAM, and the amplitude is larger than the variation in the amplitude of the EGAM. These observations suggest the importance of a different excitation mechanism from the ordinary EGAM. In the previous work[14], it has been shown that the observed behaviors of the abrupt GAM are consistent with the features of subcritical instability of the GAM which is predicted by a theoretical model proposed in Ref. [25, 26, 27]. The onset of subcritical instability requires a seed perturbation with sufficient amplitude, and the observed threshold in the amplitude of the abrupt GAM seems to correspond to the magnitude of the seed. As for the trigger for the seed, however, only the reproducibility of Lissajous diagram between the GAM and the EGAM has suggested the trigger by the EGAM. This study aims at deeper understanding the excitation mechanism of the abrupt phenomenon. Especially, the role of the EGAM is described by presenting the amplitude relation between the GAM and the EGAM as well as the phase relation.

The paper is organized as follows. In section 2, the apparatus is described. The experimental results are presented in section 3. The measured temporal evolution of the abrupt excitation phenomenon and the analysis of the phase and amplitude relations between the abrupt GAM and the EGAM will be presented. The results reveal the role of the EGAM for the abrupt excitation of the GAM. The results are summarized in section 4.

2. Apparatus

The LHD is a superconducting heliotron device with a major radius of 3.9 m and an averaged minor radius of 0.65 m[28]. In this experiment, produced plasmas have a major radius of 3.75 m and an averaged minor radius (a_{99}) of approximately 0.6 m, where the averaged minor radius is defined as the radius of a magnetic surface in which 99 % of the stored energy is included. The top view of the plasma is shown in Fig. 1 (a). The experiment has been performed under a magnetic field strength of 1.375 T. The fuel gas is hydrogen, and the plasma has been produced and sustained by a neutral hydrogen beam injection (NBI) in the counter direction with the energy of 175 keV, where "counter-direction" means that the plasma current driven by the injected beam decreases the original rotational transform of the magnetic field line. The power of the neutral beam ionized in the plasma is about 140 kW. For strong excitation of energetic particle-driven instability, a positive gradient in the high energy (supra-thermal) range of the velocity space of ions is required. Thus, in order to increase the slowing-down time of the injected beam, the electron temperature is increased by superposing electron cyclotron heating (ECH) with a power of 2.5 MW.

For measuring the toroidal mode structure of magnetic field fluctuations ($\tilde{B}_p$), six Mirnov coils are installed on the vacuum vessel of the LHD at distant toroidal locations, as shown in Fig. 1 (a). The radial profiles of the electric potential fluctuation ($\tilde{\phi}$) and the density fluctuation ($\tilde{n}$) are measured by a heavy ion beam probe (HIBP), and the measurement location moves along a curve

shown in Fig. 1 (b) by changing the injection angle of the probe beam at a frequency of 10 Hz[29, 30]. Thus, the electric potential can be measured at the normalized minor radius from -0.3 to 0.6, where minus (plus) refers to the lower (upper) of the equatorial plane of the torus. In order to measure the energy spectrum of confined ions, a neutral particle analyzer (NPA) is installed[31].

3. Experimental results

3.1. Experimental condition and typical temporal evolution

Typical waveforms of a discharge are shown in Fig. 2. The line averaged electron density is approximately 0.1×10^{19} (m^{-3}) (Fig. 2 (a)), the central electron temperature is approximately 8 ± 3 keV, and the slowing-down time of the injected beam ion (H^+) is approximately 20 s. As the result, the energy spectrum of the confined ions has a steep positive gradient below the energy of NBI[32, 33]. The temperature of the bulk ion is approximately 0.4 keV[32]. The plasma current induced by the counter NBI is lower than 3 kA which is not sufficient to change the monotonic magnetic shear.

Poloidal magnetic field fluctuations ($\tilde{B}_p$) measured by a Mirnov coil, and its spectrogram, are shown in Fig. 2(c) and (d), respectively. Figure 2 (e) and (f) show the measurement location of the HIBP and a spectrogram of the electric potential fluctuations measured by HIBP. Coherent modes with frequency up-chirping, which corresponds to evolution in the velocity space distribution function[24], from about 50 kHz to 90 kHz appear intermittently as shown by white arrows in both

$\tilde{B}_p$ (Fig. 2(d)) and $\tilde{\phi}$(Fig. 2(f)). They have been identified as an EGAM[33], and this mode is referred to as "EGAM" in the latter part of this paper. The EGAMs are observed only in low density plasmas ($< 0.3 \times 10^{19}$ (m^{-3})) in which the energetic particles do not slow down sufficiently, as shown in Ref. [33].

When the frequency of the EGAM approaches 80 kHz, another mode with half the frequency of the EGAM is abruptly and transiently excited, as marked by black arrows in Figs. 2 (d) and (f). An expanded view of $\tilde{B}_p$ is shown in Fig. 3. The duration time of the abruptly excited mode with the frequency of 41.5 kHz is less than a millisecond, and it is much shorter than the duration of the EGAM (~ 10 ms). The GAM frequency[34] calculated with parameters of the bulk plasma, when assumed to be pure hydrogen plasma, is 56 ± 10 kHz. Although the frequency of 41.5 kHz is smaller than the calculated GAM frequency, the difference can be explained by effects of energetic particles[15, 33, 35], and of impurity ions. The abruptly excited mode at 41.5 kHz has been identified as a GAM because the frequency and the spatial structures of the electric potential fluctuation and the density fluctuation associated with the mode agree with those of the GAM as shown in Ref. [14]. In this paper, this abruptly excited mode is referred to as just "GAM" in order to avoid to confuse the observed two modes, which are "EGAM " with up-chirping frequency and abruptly excited "GAM" at approximately 40 kHz.

In addition, several modes also appear at around 97 kHz, 139 kHz, and 180 kHz. The frequencies

correspond to the addition of 14 kHz to the higher harmonic frequencies of the abruptly excited GAM with frequency 41.5 kHz: $2f_d + 14 = 97$, $3f_d + 14 = 138.5$, and $4f_d + 14 = 180$, where f_d (= 41.5 kHz) is the frequency of the abruptly excited GAM. This relation between the frequencies suggests a coupling between the higher harmonics of the abrupt GAM and a mode with the frequency of 14 kHz. Because the amplitudes of the high frequency modes (> 90 kHz) are more than one order of magnitude less than those of the EGAM and of the abruptly excited GAM at 41.5 kHz, their contribution in the abrupt excitation phenomenon can be neglected.

The amplitude of $\tilde{B}_p$ associated with the abrupt GAM is typically 5 μT, and it is approximately two times larger than the maximum amplitudes of the EGAM which is 2 μT. If the abrupt excitation was caused by simple parametric coupling, the power and the frequency must satisfy the Manley-Rowe relation[36]: $P_1/f_1 = P_2/f_2$, where P and f are the power and the frequency, and the subscript indicate the coupling modes. The observed abrupt GAM and the EGAM do not satisfy this relation. Thus, the abrupt excitation is not caused by simple parametric coupling.

3.2. Nonlinear evolution of the abruptly excited GAM

A nonlinear evolution of the GAM has been observed. Figure 6 shows the temporal evolution of the amplitude of the GAM and its time derivative. The instantaneous growth rate (γ_{exp}) can be estimated as $\gamma_{exp} = \left(d\left|\tilde{B}_p\right|/dt\right)/\left|\tilde{B}_p\right|$, where $\left|\tilde{B}_p\right|$ is the amplitude of the mode.

Figure 6 (a) and (b) correspond to a case where the GAM reaches moderate amplitude. After the

GAM is triggered, the growth rate decreases monotonically as the amplitude increases. This behavior is common because the driving source is consumed by the mode excitation. In contrast, in the case that the GAM is strongly excited as shown in Fig. 6 (c) and (d), although the growth rate decreases monotonically for small amplitudes, it increases with increasing amplitude when the amplitude exceeds a threshold of approximately 2 μT. Figure 7 summarizes the relation between the growth rate and the amplitude in several events under similar experimental conditions, and it indicates the reproducibility of the threshold at approximately 2 μT in this experimental condition. This reacceleration of the growth rate cannot be explained by linear instabilities as long as the direction of the change in the driving source, such as the gradient in the phase space and the pressure gradient, does not vary in the short period. In the timescale of the GAM, the heating power of NBI and ECH is constant and the electron density is almost constant as shown in Fig. 2. Thus, the reacceleration of the growth rate is an essential nonlinear feature of the mode excitation.

3.3. Phase relation between the abruptly excited GAM and the EGAM

The abruptly excited GAM appears only in the presence of the chirping EGAM. Thus, the GAM is normally stable, and the presence of the EGAM seems to be a necessary condition for the abrupt excitation of the GAM. In order to confirm and characterize the link between the GAM and the EGAM, the phase relation between them have been investigated.

Figure 8 shows the phase difference (δ) between the abruptly-excited GAM and the EGAM during the GAM excitation, where the phase difference δ is defined as follow: $\tilde{B}_{GAM} \propto \cos(2\pi f_d t + \delta)$ for the abruptly-excited GAM with frequency f_d and $\tilde{B}_{EGAM} \propto \cos 2\pi f_2 t$ for the EGAM with frequency f_2. In order to show the reproducibility, phase difference in three events are plotted in Fig. 8, and spectrograms including the analyzed events are shown in Fig. 9 (a), (b), and (c). The phase relation shows a common tendency in the all events. If the GAM was independent from the EGAM, the phase would be random in each event. As the abrupt GAM evolves, the frequency of the EGAM rapidly changes following the second harmonic frequency of the GAM as shown in Fig. 8 (a)-(c). The specific phase relation and the change in the EGAM frequency during the GAM excitation suggests the mode coupling between the GAM and the EGAM, though a simple parametric coupling cannot explain the abrupt excitation as described in section 3.1. This coupling also cannot be explained by known driving mechanisms of the GAM, such as nonlinear coupling of turbulence[37] and the inverse Landau damping by energetic particles[15].

3.4. Relation between the amplitude of the EGAM and excitation of the GAM

In the previous section, it is revealed that the EGAM is related to the abrupt excitation of the GAM. If the EGAM plays an essential role, the GAM excitation will correlate with the amplitude of the EGAM. Figure 9 shows the relation between the amplitude of the GAM and the amplitude of the EGAM, where the latter amplitude is measured just before the abrupt GAM excitation. It indicates

that the GAM is not excited if the amplitude of the EGAM is smaller than 1.2 μT. Thus, there is a threshold in the amplitude of the EGAM for the abrupt excitation of the GAM.

Note that, even if the amplitude of the EGAM exceeds the threshold, the GAM is not excited in some cases. That suggests existence of other parameters determining the abrupt GAM excitation, and it will be discussed in the next section..

4. Discussion

The experimental results indicate that the abrupt excitation of the GAM involves a coupling with the EGAM with up-chirping frequency. However, the coupling cannot be explained by a simple parametric coupling and know driving mechanisms of the GAM, such as nonlinear coupling of turbulence and the inverse Landau damping, as described above.

According to a theoretical model proposed in Ref [25, 26, 27], a subcritical instability of the GAM can be driven by a cooperative collaboration of kinetic nonlinearity, which corresponds to resonant interactions between GAM and energetic particles, and fluid nonlinearity, which corresponds to nonlinear parametric coupling between the EGAM(mother mode) and the GAM (daughter mode). Thus, the abrupt excitation phenomenon can be interpreted as the subcritical instability of the GAM(daughter mode) triggered by the chirping EGAM(mother mode), and the energy of the instability comes from the EGAM (mother mode) and the energetic particle. The time scales of the GAM excitation, the phase relation and amplitude relation between the GAM and the

EGAM are reproduced by the model as shown in Ref. [25]. Recently, another simulation by MEGA code[38, 35] which is a hybrid simulation code taking into account kinetic energetic particles and a MHD fluid shows that the coupling between the GAM and the EGAM arises only from a kinetic coupling via energetic particles[39]. Although the amplitude of the excited GAM is much smaller than that of the EGAM in the simulation unlike the experimental results at present, Ref. [39] indicates the kinetic coupling induced by resonant interaction between the EGAM and energetic particles causes the GAM oscillation, and the coupling may become a trigger of the subcritical instability with the large amplitude if the sufficient seed to exceed a threshold for the subcritical instability is given. Thus, both the candidate theories don't contradict the interpretation that the observed relation between the GAM and the EGAM indicate that the EGAM triggers the abrupt GAM excitation, though the coupling mechanism triggering the instability has not been identified, yet.

The excitation of a subcritical instability requires a seed with sufficient amplitude and a trigger. The threshold in the amplitude of the GAM (Fig. 7) can be interpreted as the required amplitude of the seed, and the threshold in the amplitude of the EGAM (Fig. 9) can be interpreted to correspond to the threshold in the trigger. Thus, the experimental results indicate that the abrupt excitation phenomenon has the nature of the subcritical instability.

The scattering data in Fig. 9 can be explained by the theoretical model in Ref. [26]. According to

the theoretical model, the threshold has been analytically predicted as $D^2 \geq d\theta/dt$, where D is proportional to the amplitude of the EGAM, and $d\theta/dt$ is the frequency chirping rate of the EGAM if the linear growth rate of the GAM is small. Thus, the theory predicts that the excitation condition is determined not only by the magnitude of the EGAM but also by the frequency chirping rate of the EGAM. In other words, the threshold in the amplitude of the EGAM for the abrupt GAM excitation depends on the frequency chirping rate of the EGAM. Figure 10 is a summary of the parameters (amplitudes and chirping rate) where the abrupt GAM is excited. Here, the analyzed data are the same as those in Fig. 9. The excitation boundary seems to agree with the theoretical prediction on the excitation threshold, which is $D^2 \geq d\theta/dt \propto df/dt$, qualitatively.

The threshold in the trigger (Fig. 9) and the threshold in the amplitude (Fig. 7) are the essential features of a subcritical instability, and the theoretical prediction of the parameter dependence of the threshold agrees with the experimental result (Fig. 10). Therefore, the observed abrupt phenomenon can be interpreted as the excitation of the subcritical instability of the GAM.

5. Summary

Abrupt excitation of a GAM has been found in the LHD, when the frequency of the chirping EGAM approaches twice the GAM frequency. The phase relation between the GAM and the EGAM is common to all excitation events, and it indicates mode coupling between the GAM and the EGAM.

However, the relation between amplitude variations of the abrupt GAM with the lower frequency and the EGAM with the higher frequency does not satisfy the Manley-Rowe relation. Thus, although mode coupling is involved, it does not explain the abrupt excitation.

The observed characteristics of the abrupt excitation of the GAM, such as the phase, the amplitude, and time scales of the evolution, can be explained by a theoretical model[25, 26, 27], which shows that a subcritical instability of the GAM can be driven by a cooperative collaboration between kinetic nonlinearity and fluid nonlinearity. The observed threshold in amplitude of the GAM for the reacceleration of the growth rate seems to correspond to the threshold in the magnitude of the seed required for the growth of the subcritical instability, and the threshold in the amplitude of the EGAM for the GAM excitation seems to correspond to the threshold in the magnitude of the trigger. Thus, the observed thresholds indicate that the abrupt excitation phenomenon of the GAM with a large amplitude has a nature of a subcritical instability, and this experiment would be the first demonstration of the presence of subcritical instability in magnetically confined plasmas. Since a subcritical instability is one of the working hypotheses[1] of the onset of abrupt phenomena such as sawtooth oscillation and disruption in laboratory plasmas and solar flare in astro-plasmas, this study identifies an experimental path to explore the trigger problem of abrupt phenomena.

Acknowledgement

The authors thank Dr. H. Wang and Prof. Y. Todo of National Institute for Fusion Science and Dr. N. Yokoi of University of Tokyo for useful discussions and the LHD Technical Group for its support. They are also grateful to Dr. K. Hallatschek of Max-Planck-Institute for Plasma Physics and Dr. K. Shinohara of National Institutes for Quantum and Radiological Science and Technology for their valuable comments. This work was supported by MEXT Japan under Grant-in-Aid for Scientific Research (A) (No. 15H02155), (C) (No. 24561031, 15K06653), for Challenging Exploratory Research (No. 24656561, 16K13923), for Young Scientists (B) (No. 15K18305), NIFS/NINS under NIFS10ULHH020 and NIFS10ULHH023, and the Collaborative Research Program of Research Institute for Applied Mechanics, Kyushu University.

Reference

[1] ITOH, S., ITOH, K., ZUSHI, H., and FUKUYAMA, A., Plasma Phys. Control. Fusion **40** (1998) 879.

[2] BHATTACHARJEE, A., MA, Z. W., and WANG, X., *Lecture Notes in Physics 614: Turbulence and Magnetic Fields in Astrophysics*, Springer, Berlin, 2003.

[3] YAGI, M., ITOH, S.-I., ITOH, K., FUKUYAMA, A., and AZUMI, M., Phys. Plasma **2** (1995) 4140.

[4] CARRERA, R., HAZELTINE, R., and KOTSCHENREUTHER, M., Phys. Fluids **29** (1986) 899.

[5] O'NEIL, T., Phys. Fluids **10** (1967) 1027.

[6] DUPREE, T. H., Phys. Fluids **25** (1982) 277.

[7] DUPREE, T. H., The Physics of fluids **26** (1983) 2460.

[8] BERK, H., BREIZMAN, B., CANDY, J., PEKKER, M., and PETVIASHVILI, N., Phys. Plasma **6** (1999) 3102.

[9] LESUR, M., IDOMURA, Y., and GARBET, X., Phys. Plasma **16** (2009) 092305.

[10] LESUR, M., IDOMURA, Y., SHINOHARA, K., and GARBET, X., pop **17** (2010) 122311.

[11] NGUYEN, C., GARBET, X., GRANDGIRARD, V., et al., Plasma Phys. Control. Fusion **52** (2010) 124034.

[12] LESUR, M., DIAMOND, P. H., and KOSUGA, Y., Plasma Phys. Control. Fusion **56** (2014) 075005.

[13] WINSOR, N., JOHNSON, J. L., and DAWSON, J. M., Phys. Fluids **11** (1968) 2448.

[14] IDO, T., ITOH, K., OSAKABE, M., et al., Phys. Rev. Lett. **116** (2016) 015002.

[15] FU, G., Phys. Rev. Lett. **101** (2008) 185002.

[16] BOSWELL, C., BERK, H., BORBA, D., et al., Phys. Lett. A **358** (2006) 154.

[17] BERK, H., BOSWELL, C., BORBA, D., et al., Nucl. Fusion **46** (2006) S888.

[18] NAZIKIAN, R., FU, G., AUSTIN, M., et al., Phys. Rev. Lett. **101** (2008) 185001.

[19] TOI, K., WATANABE, F., TOKUZAWA, T., et al., Phys. Rev. Lett. **105** (2010) 145003.

[20] IDO, T., SHIMIZU, A., NISHIURA, M., et al., Nucl. Fusion **51** (2011) 073046.

[21] MATSUNAGA, G., KAMIYA, K., SHINOHARA, K., MIYATO, N., and KOJIMA, A., Proc. the 39th EPS Conf. on Plasma Phys. Stockholm, 2-6 July (2012) P2.062 (http://ocs.ciemat.es/epsicpp2012pap/pdf/P2.062.pdf).

[22] LAUBER, P., CURRAN, D., SCHNELLER, M., et al., 13th IAEA Technical Meeting on Energetic Particles in Magnetic Confinement Systems, Beijing, China (2013).

[23] CHEN, W., DING, X., YU, L., et al., Phys. Lett. A **377** (2013) 387.

[24] BERK, H., BREIZMAN, B., and PETVIASHVILI, N., Phys. Lett. A **234** (1997) 213.

[25] LESUR, M., ITOH, K., IDO, T., et al., Phys. Rev. Lett. **116** (2016) 015003.

[26] ITOH, K., ITOH, S. I., KOSUGA, Y., LESUR, M., and IDO, T., Plasma Physics Reports **42** (2016) 418.

[27] LESUR, M., ITOH, K., IDO, T., et al., Nucl. Fusion **56** (2016) 056009.

[28] IIYOSHI, A., KOMORI, A., EJIRI, A., et al., Nucl. Fusion **39** (1999) 1245.

[29] IDO, T., SHIMIZU, A., NISHIURA, M., et al., Rev. Sci. Instrum. **77** (2006) 10F523.

[30] SHIMIZU, A., IDO, T., NISHIURA, M., and KATO, S., Plasma Fusion Res. **5** (2010) S1015.

[31] OSAKABE, M., YAMAMOTO, S., TOI, K., et al., Nucl. Fusion **46** (2006) S911.

[32] OSAKABE, M., IDO, T., OGAWA, K., et al., Proc. of the 25th IAEA Fusion Energy Conference (2014) Ex/10-3 (http://www.nifs.ac.jp/report/IAEA2014/EX-10-3_Osakabe.pdf) .

[33] IDO, T., OSAKABE, M., SHIMIZU, A., et al., Nucl. Fusion **55** (2015) 083024.

[34] SUGAMA, H. and WATANABE, T., Phys. Plasma **13** (2006) 012501.

[35] WANG, H., TODO, Y., IDO, T., and OSAKABE, M., Phys. Plasma **22** (2015) 092507.

[36] MANLEY, J. M. and ROWE, H. E., Proceedings of the IRE **44** (1956) 904.

[37] DIAMOND, P. H., ITOH, S.-I., ITOH, K., and HAHM, T., Plasma Phys. Control. Fusion **47** (2005) R35.

[38] TODO, Y., BERK, H., and BREIZMAN, B., Nucl. Fusion **50** (2010) 084016.

[39] WANG, H., TODO, Y., and SUZUKI, Y., Proc. of the 26th IAEA Fusion Energy Conference (2016) TH/P4-11 (https://conferences.iaea.org/indico/event/98/session/22/contribution/565/material/paper/0.pdf) .

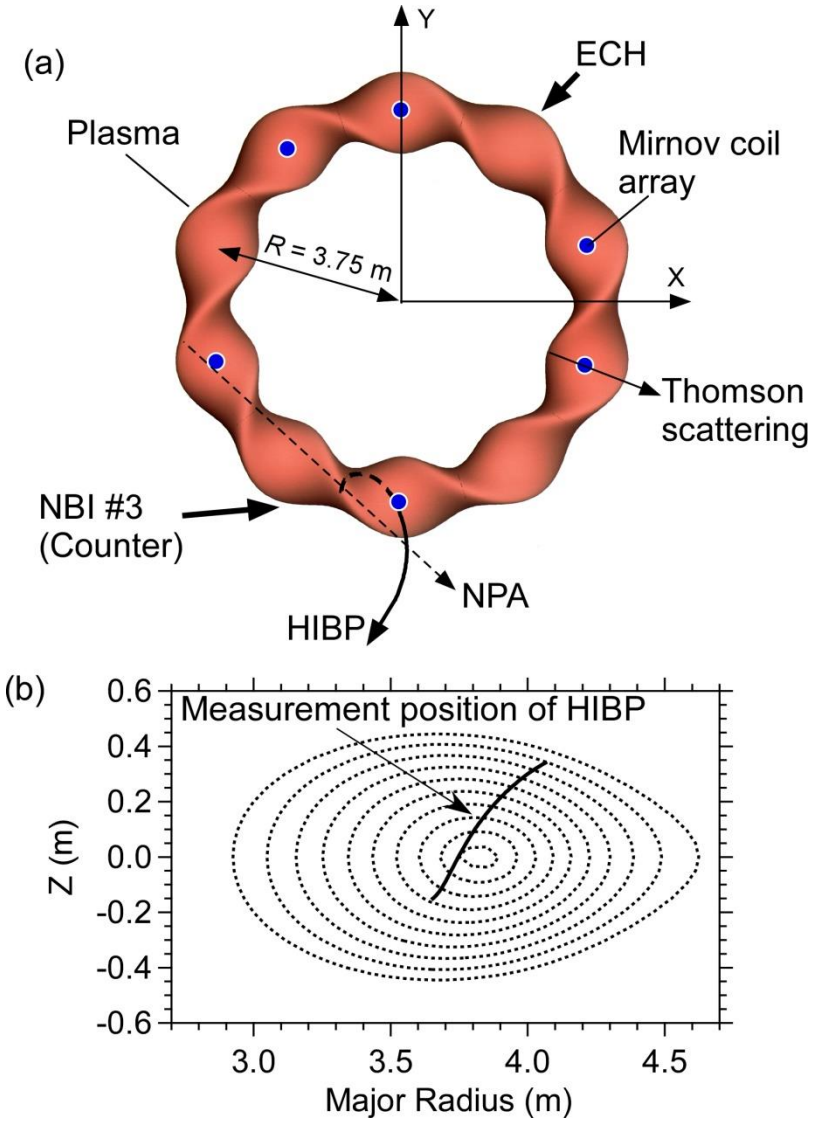

Fig. 1 (a) Top view of LHD plasma and layout of heating and diagnostic equipment. (b) Measurement location of the HIBP during a sweep of the probe beam. The nested dotted contours are poloidal cross sections of magnetic surfaces calculated by the VMEC code [S. P. Hirshman, et al., Comp. Phys. Comm., 43, 143 (1986)].

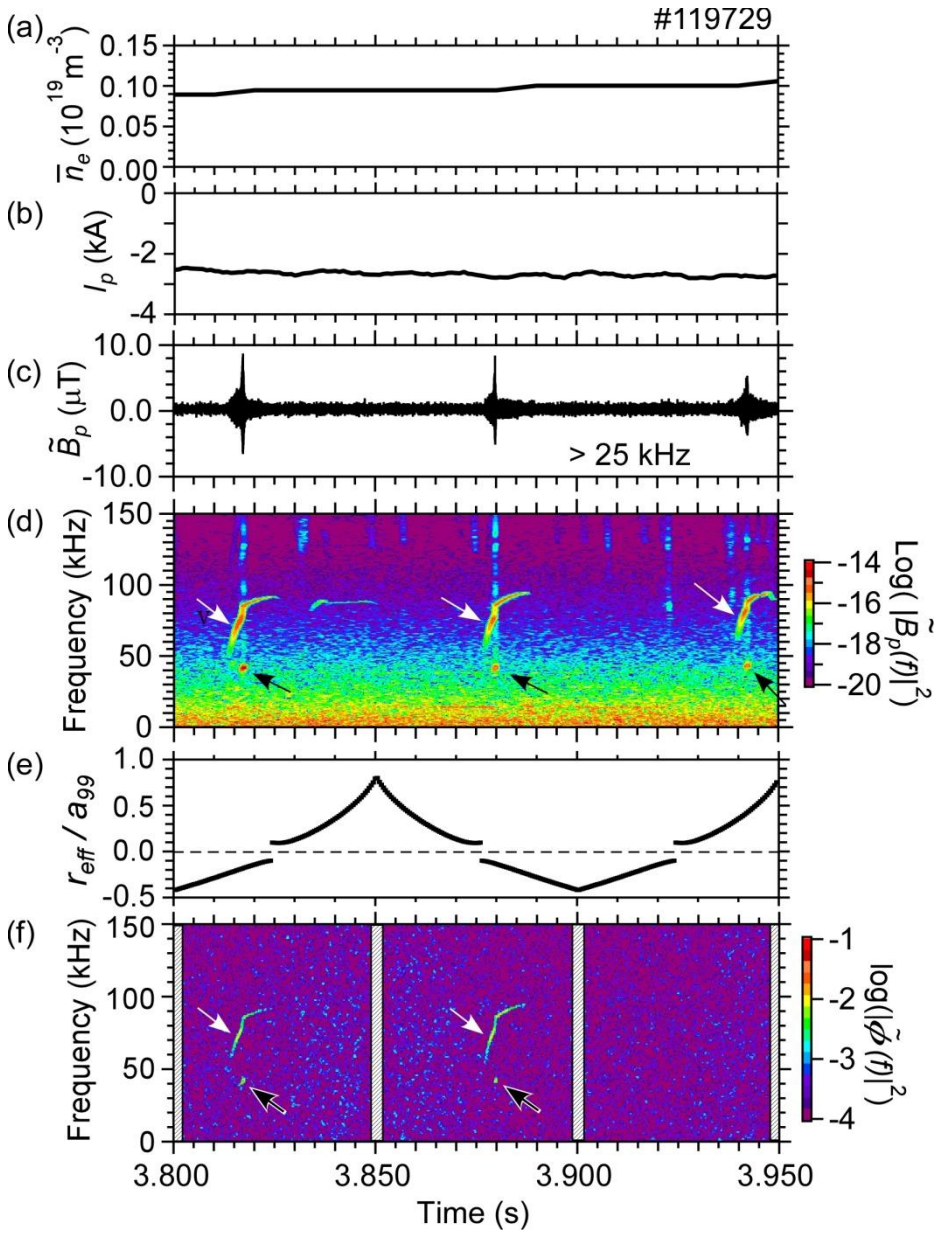

Fig. 2 (a) Line averaged electron density. (b) Plasma current. (c) Magnetic field fluctuations measured by a Mirnov coil, and (d) its spectrogram. (e) Measurement location of the HIBP, where r_{eff} is the averaged minor radius, and a_{99} is the averaged minor of a magnetic flux surface which includes 99 % of the stored energy. (f) Spectrogram of the electric field fluctuation measured by the HIBP. White and black arrows indicate EGAM and abruptly excited GAM, respectively.

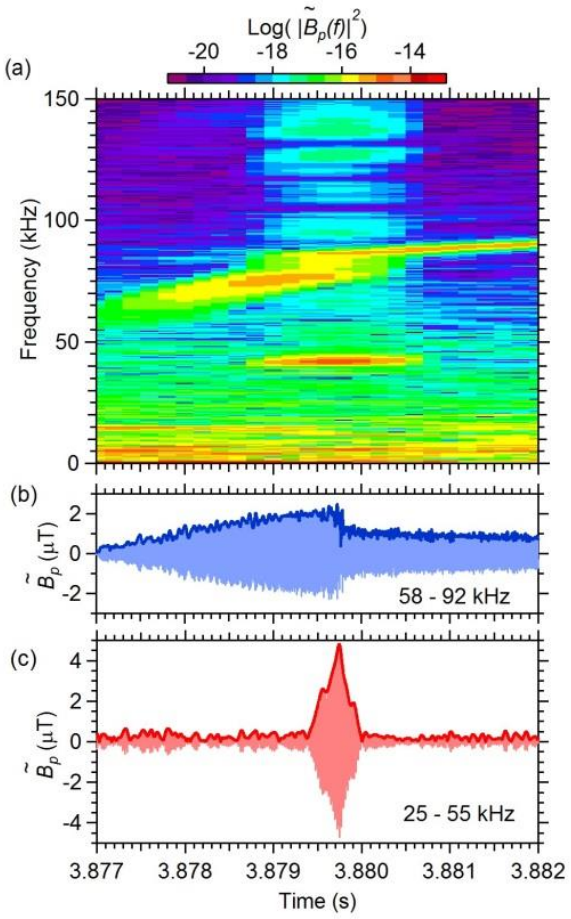

Fig. 3 (a) Spectrogram of the magnetic field fluctuations ($\tilde{B}_p$). (b) and (c) show waveforms extracted by using numerical band-pass filters with the pass band of 58 - 92 kHz and 25 - 55 kHz, respectively. The former (b) corresponds to the EGAM and the latter (c) corresponds to the abruptly excited mode. Bold curves show the envelopes.

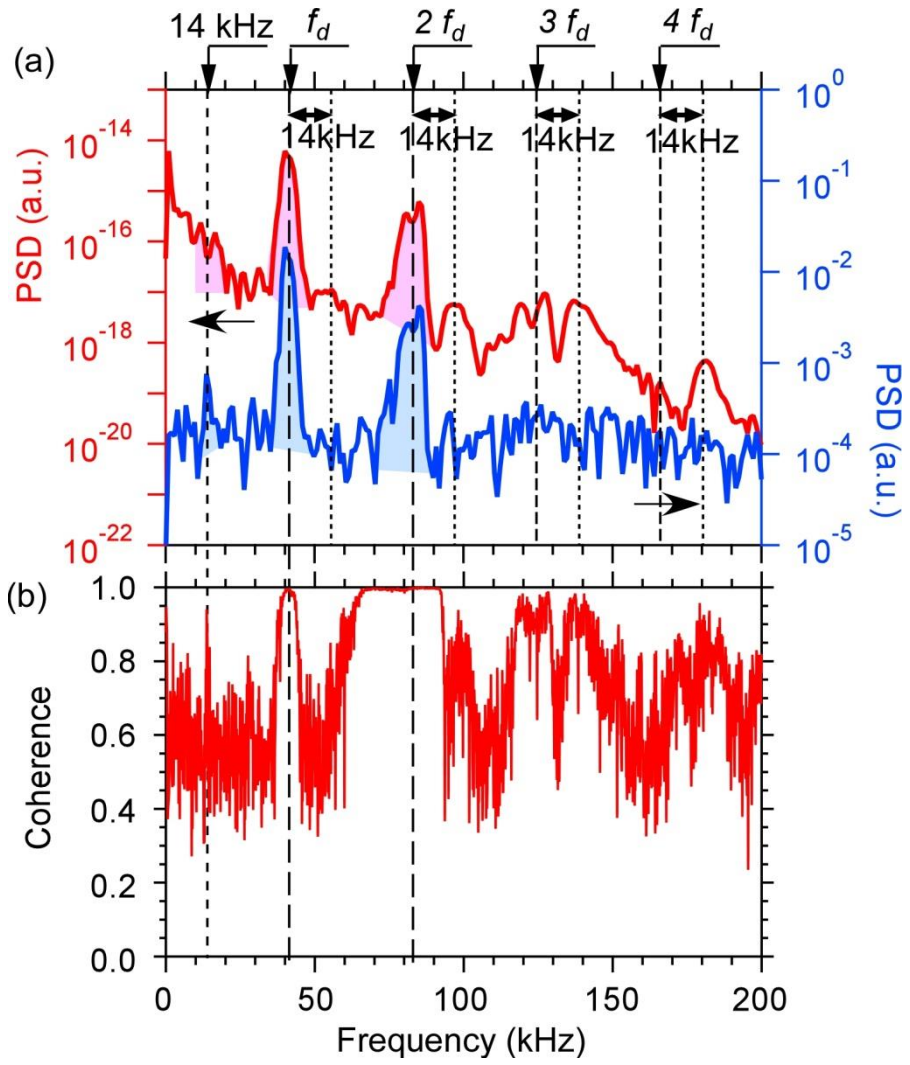

Fig. 4 (a) Frequency spectra of the magnetic field fluctuation and the electric potential fluctuation. (c) Coherence between magnetic field fluctuations measured by Mirnov coils aligned in the toroidal direction.

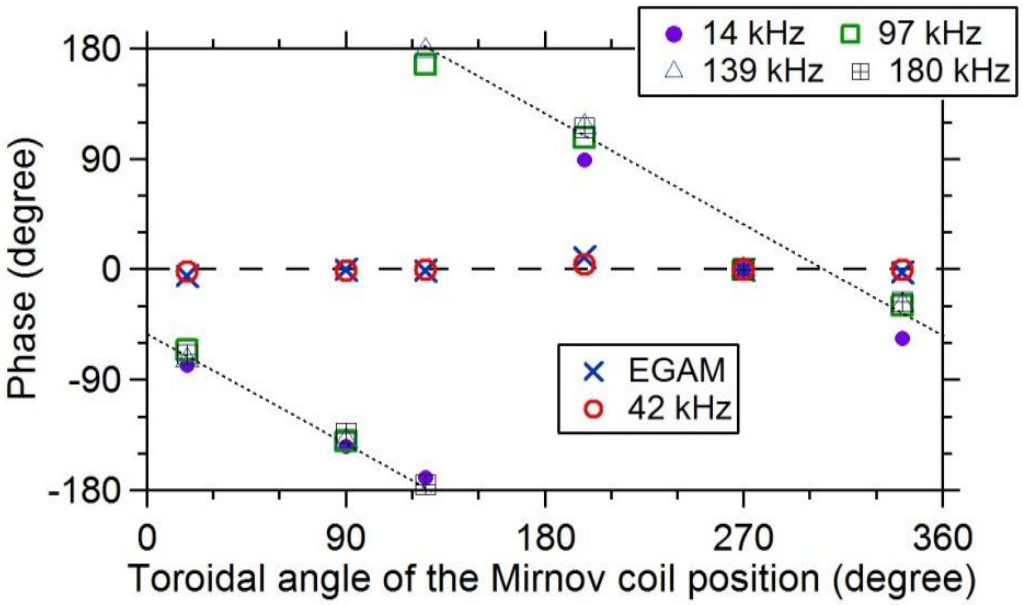

Fig. 5 Phase of the magnetic field fluctuations. The horizontal axis is the toroidal angle of the position of the Mirnov coils.

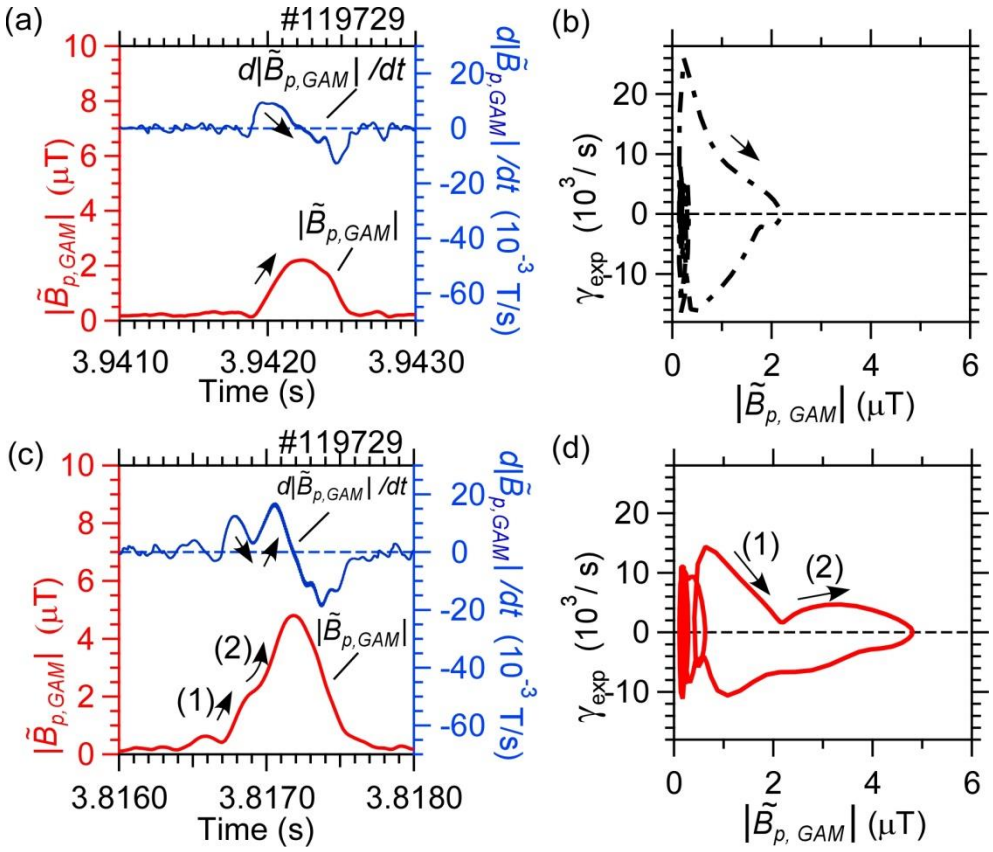

Fig. 6 Growth rate of the GAM. (a) and (c) Typical temporal evolution of the amplitude associated with the GAM($|\tilde{B}_{p,GAM}|$), and its time derivative. (b) and (d) Amplitude dependence of the time-dependent growth rate estimated as $\gamma_{\exp} = \left(d|\tilde{B}_{p,GAM}|/dt\right)/|\tilde{B}_{p,GAM}|$. (b) and (d) correspond to the periods of (a) and (c), respectively.

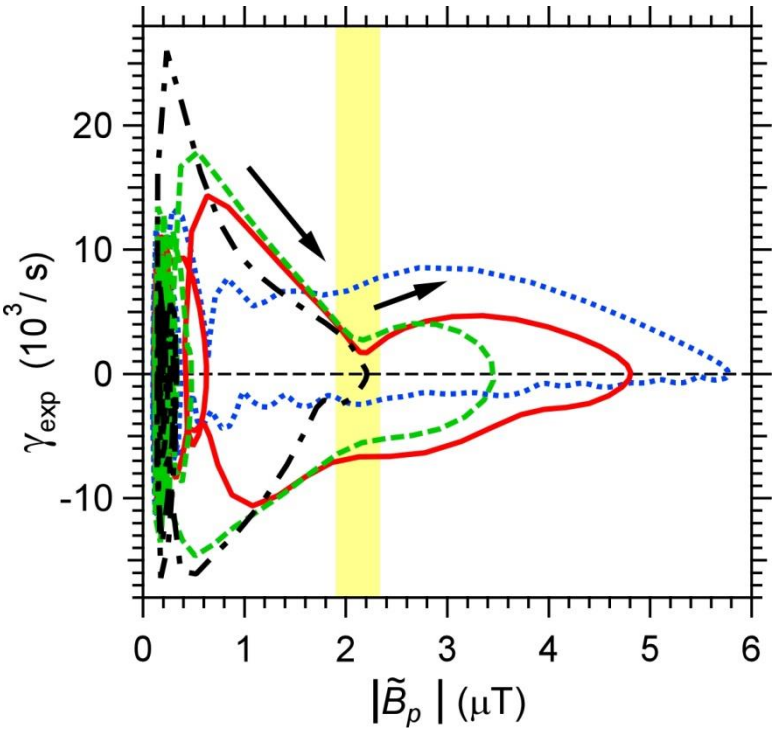

Fig. 7 Amplitude dependence of the growth rate in 4 bursts of the GAM.

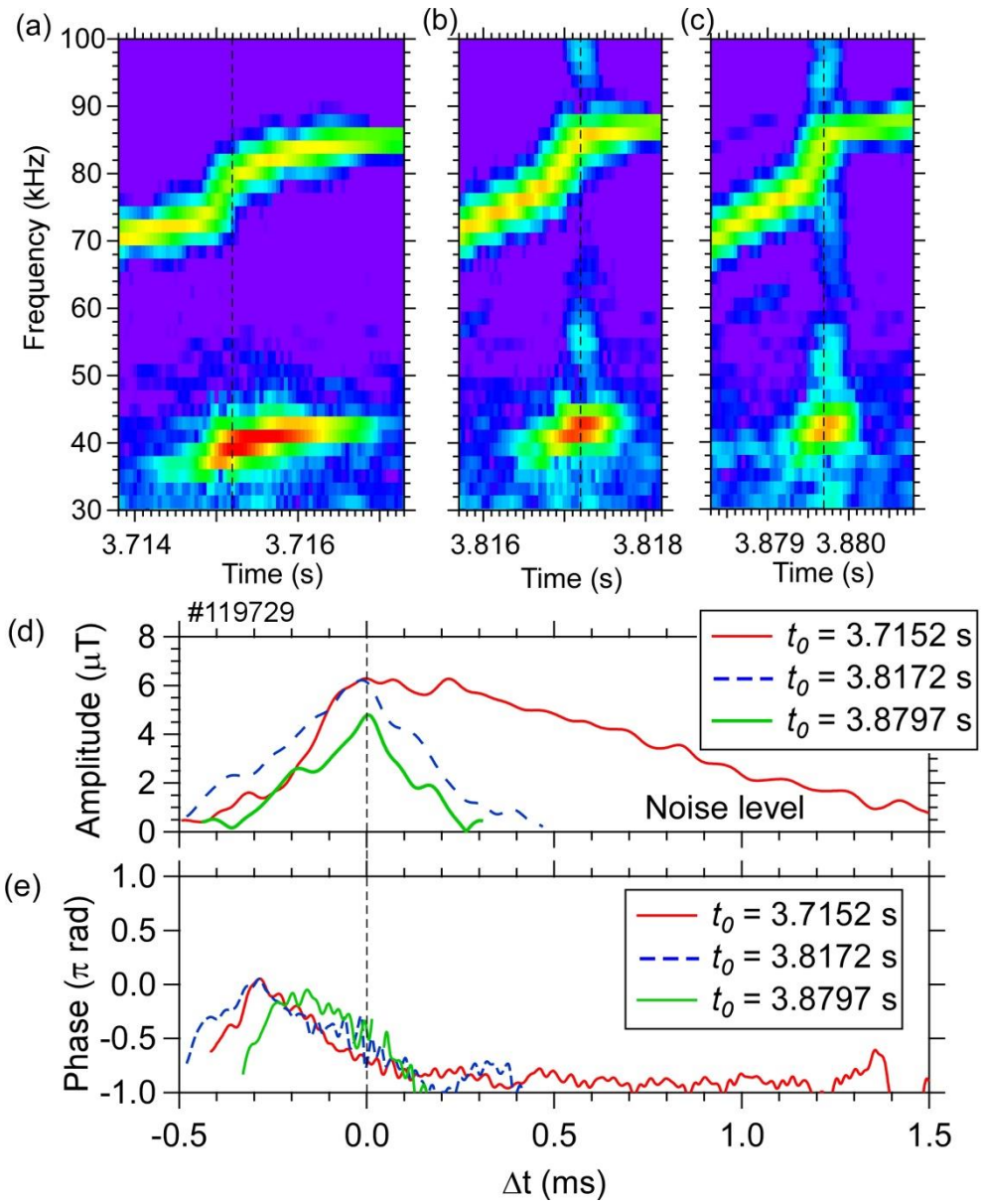

Fig. **8** (a), (b), and (c) Expanded view of spectrograms of the magnetic field fluctuation. The time windows used in FFT is 0.512 ms (256 samples) The dashed lines indicate the time of maximum GAM amplitude(t_0). (d) Temporal evolution of the amplitude of the abrupt GAMs. The origin of the horizontal axis indicates the time of maximum GAM amplitude. (e) Phase difference (δ) between the GAM and the EGAM. In the case that $\tilde{B}_{EGAM} \propto \cos 2\pi f_2 t$ for the EGAM, the GAM is expressed as $\tilde{B}_{GAM} \propto \cos(2\pi f_d t + \delta)$ with the phase δ.

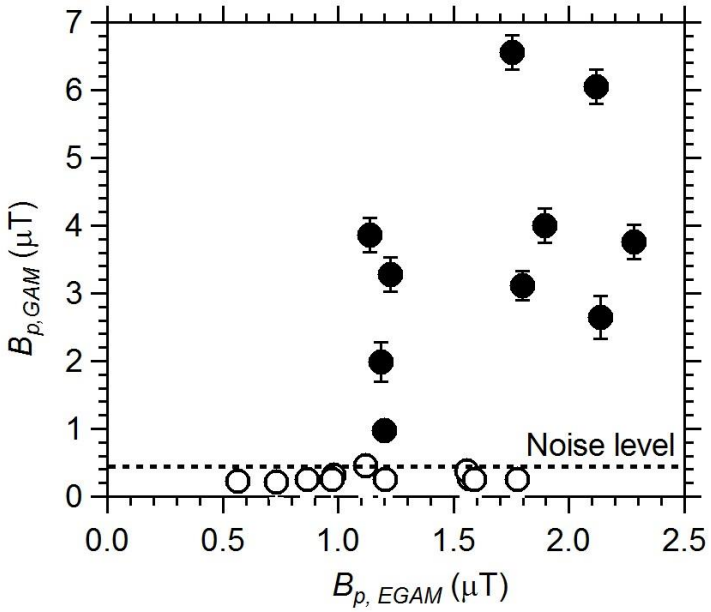

Fig. 9 Relation between the amplitude of the EGAM (horizontal axis) and the amplitude of abruptly-excited GAM (vertical axis). In the case that the abrupt GAM is apparent (filled circles), the amplitude of the EGAM is measured just before the onset of the GAM, and the amplitude of the GAM is its maximum amplitude. In the case that the presence of abrupt GAM is unclear (open circles), the amplitude of the EGAM is measured at the same frequency as the other EGAMs accompanied by an abrupt GAM under similar experimental condition.

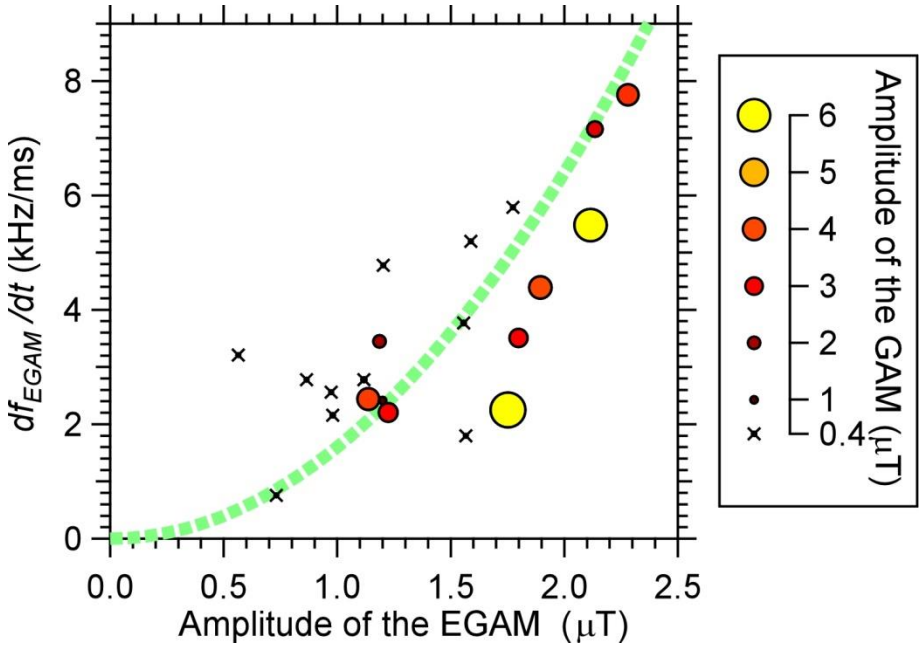

Fig. 10 Parameters in which abrupt GAMs are excited. The horizontal axis is the amplitude of the EGAM, and the vertical axis is the chirping rate of the EGAM. The data are the same as those in Fig. 9. Size of the markers indicates amplitude of excited GAM, and the noise level is at 0.4 μT. The dotted curve shows $df_{EGAM}/dt \propto \left|\tilde{B}_{\mathrm{p,EGAM}}\right|^2$, as an eye guide.